Quarterly Progress Report

N01-NS-1-2333

Restoration of Hand and Arm Function by Functional Neuromuscular Stimulation

Period covered: January 1, 2003 to March 31, 2003

Principal Investigator: Robert F. Kirsch, Ph.D.

Co-Investigators:

Patrick E. Crago, Ph.D.	Joseph M. Mansour, Ph.D.
P. Hunter Peckham, Ph.D.	Jeffrey L. Duerk, Ph.D.
Warren M. Grill, Ph.D.	Wyatt S. Newman, Ph.D.
J. Thomas Mortimer, Ph.D.	Harry Hoyen, M.D.
Kevin L. Kilgore, Ph.D.	John Chae, M.D.
Michael W. Keith, M.D.	Jonathon S. Lewin, M.D.
David L. Wilson, Ph.D.	Dustin Tyler, Ph.D.
Dawn Taylor, Ph.D.	

Program Manager: William D. Memberg, M.S.

Case Western Reserve University
Wickenden 407
10900 Euclid Avenue
Cleveland, OH 44106-7207
216-368-3158 (voice)
216-368-4969 (FAX)
rfk3@po.cwru.edu

Contract abstract

The overall goal of this contract is to provide virtually all individuals with a cervical level spinal cord injury, regardless of injury level and extent, with the opportunity to gain additional useful function through the use of FNS and complementary surgical techniques. Specifically, we will expand our applications to include individuals with high tetraplegia (C1-C4), low tetraplegia (C7), and incomplete injuries. We will also extend and enhance the performance provided to the existing C5-C6 group by using improved electrode technology for some muscles and by combining several upper extremity functions into a single neuroprosthesis. The new technologies that we will develop and implement in this proposal are: the use of nerve cuffs for complete activation in high tetraplegia, the use of current steering in nerve cuffs, imaging-based assessment of maximum muscle forces, denervation, and volume activated by electrodes, multiple DOF control, the use of dual implants, new neurotization surgeries for the reversal of denervation, new muscle transfer surgeries for high tetraplegia, and an improved forward dynamic model of the shoulder and elbow. During this contract period, all proposed neuroprostheses will come to fruition as clinically deployed and fully evaluated demonstrations.

Summary of activities during this reporting period

The following activities are described in this report:
- *Measurement of human upper extremity nerve diameters and branch-free lengths*
- *Nerve cuff electrode fabrication*
- *Design of an EOG-based command interface for prosthetic control*
- *Real-time control of neural prostheses*
- *Testing of stimulation artifact suppression technique and protocols to be used in percutaneous implementation of a myoelectric controlled neuroprosthesis*
- *An integrated voluntary muscle and FES controller to restore elbow extension in spinal cord injury*

Measurement of human upper extremity nerve diameters and branch-free lengths.

Contract sections:
E.1.a.i Achieving Complete and Selective Activation Via Nerve Cuff Electrodes
E.2.a.i Selective Activation of Elbow and Shoulder Muscles by Nerve Cuff Electrodes

Introduction
The ability to selectively activate peripheral nerve trunk fascicles using nerve cuff electrodes is well established. In the effort to combine several upper extremity functions into a single neuroprosthesis it is desirable to use this technology for specific muscle activations. External and internal topography studies of the upper extremity nerves are necessary so that implant sites which maximize stimulation success can be identified. The external study has been previously reported upon and included measurements of the diameters and branch free lengths of the target nerves in six complete brachial plexus dissections. The results of this study indicated acceptable diameters and branch free lengths at the targeted cuff sites. The goal of the internal

study is to obtain accurate fascicle topographies at the targeted areas so that computer simulations of the stimulation patterns may be implemented. To increase the amount of information obtained from the internal studies, the use of lipophilic dyes that retrogradely diffuse in fixed nerve tissue is being investigated. A method to enhance the diffusion rates of these dyes via application of dc electric fields has demonstrated promise.

Internal Study Results

Traditional cross-sectioning is largely ineffective as a means to follow fascicles through the length of a nerve. Figure 1 shows the degree of change that can be seen in peripheral nerve topography over relatively short distances and illustrates the difficulty in matching patterns from cross-section to cross-section. Even with high frequency cross-sectioning mapping fascicles from one slide to the next is, at best, a process of repeated educating guessing that cannot preclude errors. Furthermore, traditionally cross-sectioning reveals no information about the location of functional groups at a sub-fascicular level. These limiting factors led us to attempt to use a set of lipophilic dyes that has previously been shown to trace fixed nerve fibers.

Figure 1. Radial nerve cross-sections 4mm apart.

Retrograde tracing utilizing lipophilic dyes has been used in postmortem formaldehyde fixed nerve fibers [Honig and Hume 1986, 1989; Godement et al. 1987; Honig 1993]. The main limitation of these dyes is the limited maximal tracing distance that can be achieved due to the slow diffusion in fixed tissue. This slow diffusion rate is due to the cross-linking of proteins that occurs during the aldehyde fixation process [Sparks et al. 2000]. Lukas et al. found maximal tracing distance for DiI (1,1'-dioctadecyl-3,3,3'3'-tetramethlylindocarbocyanine perchlorate), DiO (3,3'-dioctadecyloxa-carbocyanine perchlorate), and DiA (4-(4-dihexadecylamino)styryl)-n-methylpyridinium iodide) in fixed human tissue. Their results found that incubation at 37°C for 12-15 weeks provided maximal tracing distances of 28.9 ±2.2 mm for DiI with DiO and DiA having maximal tracing distances varying from 15 to 20 mm.

Lukas's optimal distances are consistent with other reports and fall well below the distances that would be necessary for our needs. In the radial nerve, tracing distances of at least 200 mm are required to identify the location of muscle branches that are targeted for selective activation at the cuff electrode implantation sites. To overcome this diffusion rate limitation, a method to enhance the diffusion rates of these dyes has been developed so that maximal tracing distances can be greatly extended.

This method hinges upon the fact that these three dyes (DiI, DiO, and DiA) as well as an additional analog (DiR) are all positively charged molecules. Theoretically, application of dc fields across the dye loaded nerve tissue should result in greater diffusion values then previously reported. To test this theory, two studies were performed. The first of these studies was a constant-field, time-variant study, and the second study was a field-variant, constant-time study.

DiI, dissolved in ethanol at a ratio of 1 mg/ml, was applied via a micropipette to a triangular cross-section made 1 cm from the end of a 6 cm nerve sample taken from human median or ulnar nerves. Platinum plate electrodes were positioned at either end of the nerve sample with the electrode closer to the initial DiI loading site serving as the anode. A dc electric field of 40 V/cm was applied across the tissue for times of 12, 24 and 48 hours. Following, this tracing period the nerve sample was cross-sectioned to reveal the extent of DiI diffusion.
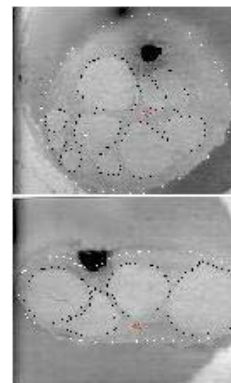
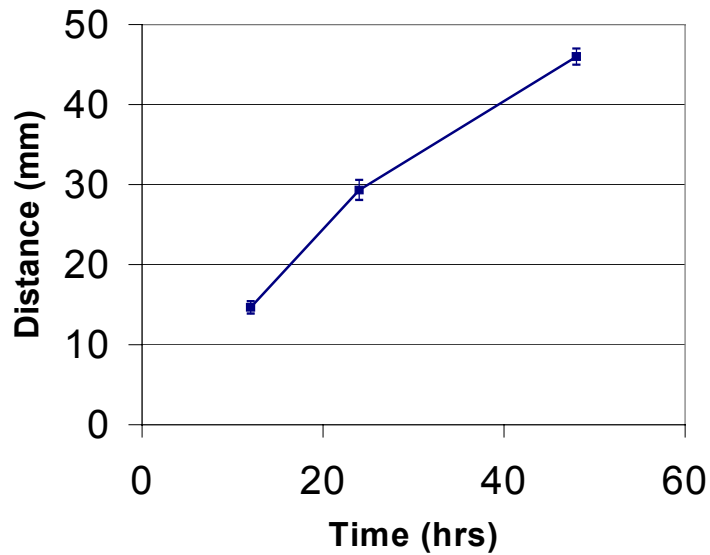## One Field Strength, Multiple Tracing Times
(40 V/cm)

Figure 2. Results of a multiple tracing time, constant-field strength study. Shows effect of a 40 V/cm applied electric field on the diffusion distance of DiI in fixed peripheral nerve tissue.

Multiple field strengths, constant tracing time
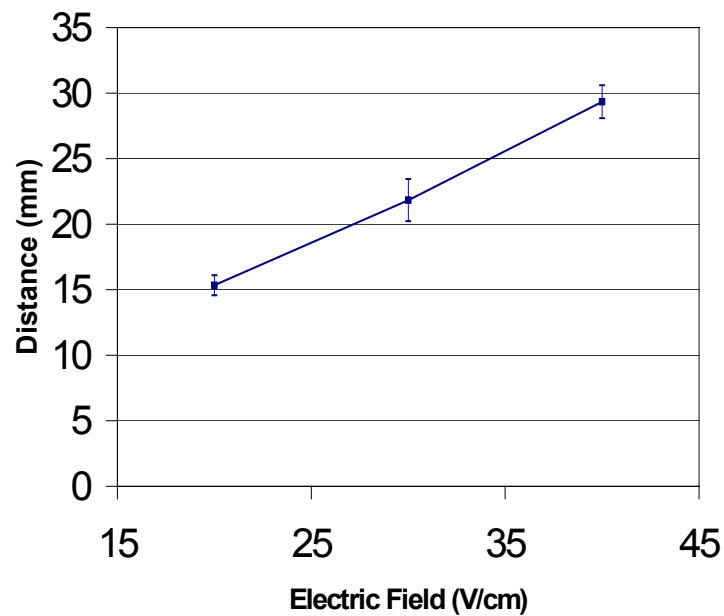## (24 hours)

Figure 3. Results of a multiple field strength, constant-tracing time study for DiI in fixed peripheral nervous tissue.

Figure 2 shows the results of this study. The mean velocity value for the entire study was 1.13 mm/hr. This corresponds to a 98.3 times increase in diffusion velocity over reported non-enhanced tracing values. A maximum tracing distance of 47 mm was reached in 48 hours which corresponds to a 1.6 times improvement over the previously reported maximum.

The second study performed was a field-variant, constant-time study. Using the same dye application method, DiI loaded nerves were subject to field strengths of 20, 30, and 40 V/cm for a period of 24 hours. Figure 3 shows the results of this study. The average tracing distance observed after 24 hours was 15.3 mm for a 20 V/cm field, 21.8 mm for a 30 V/cm field and 29.3 mm for a 40 V/cm field. The results of these tracing experiments illustrate a method that overcomes the diffusion rate limitations of the lipophilic dyes in fixed tissue. This tool will allow us to create accurate fascicle maps over long distances of peripheral nerves with up to four branches of a nerve being distinctly labeled.

Next Quarter

The use of applied dc fields to overcome diffusion limitations for DiI in fixed peripheral nervous tissue will allow us to create accurate fascicular maps of targeted muscle groups. Extension of this electric field technique to analogous neural tracers (DiO, DiA, and DiR) will allow the possibility for up to four branches to be distinctly tagged within a main nerve trunk. The results of these tracing studies will reveal novel insight into the functional grouping of branches in proximal locations of main nerve trunks.

References

Godement P, Vanselow J, Thanos S and Bonhoeffer F. (1987) A study in the developing visual systems with a new method of staining neurones and their processes in fixed tissue, Development, 101:697-713.

Honig MG and Hume RI. (1986) Fluorescent carbocyanine dyes allow living neurons of identified origin to be studied in long-term cultures, J. Cell Biol., 103:171-187.

Honig MG and Hume RI. (1989) DiI and DiO: versatile fluorescent dyes for neuronal labeling and pathway tracing, Trends Neurosci., 12:333-341.

Lukas JR, Aigner M, Denk M., Heinzl H, Burian M, and Mayr R. (1998) Carbocyanine Postmortem Neuronal Tracing: Influence of Different Parameters on Tracing Distance and Combination with Immunocytochemistry, J. Histo Cyto, 46(8):901-10.

Sparks DL, Lue L, Martin TA, and Rogers J. (2000) Neural tract tracing using Di-I: a review and a new method to make fast Di-I faster in human brain, J. Neur Meth, 103:3-10.

Nerve Cuff Electrode Fabrication

Contract section:
E.1.a.i   Achieving Complete and Selective Activation Via Nerve Cuff Electrodes

Introduction
Self-sizing spiral nerve cuff electrodes [Naples, et. al., 1988] will be utilized to achieve complete activation of shoulder muscles in individuals with high tetraplegia. These electrodes have been used extensively in animal studies and have also been used on the human optic nerve [Veraart, et. al. 1998]. Single- and multi-contact cuff electrodes will initially be evaluated via a percutaneous lead, after which the cuffs will be connected to an implanted stimulator.

Fabrication Progress
During the past quarter, we procured the necessary materials for fabrication of cuff electrodes, and began drafting the fabrication protocols for both the individual cuff electrode components *and* the entire cuff electrode. This included the development of a branching section of the lead that takes the four-conductor lead from the cuff and splits it into four single-conductor leads with connectors. In addition, we commenced a rigorous risk analysis of the cuff electrode design in order to identify areas where additional quality assurance inspections during the fabrication process will ensure delivery of a reliable, robust, and inherently safe cuff electrode.
We are in the midst of refining the cuff electrode fabrication protocols through the fabrication and examination of cuff electrode prototypes. Once finalized, the fabrication protocols will be validated to ensure consistency across electrodes during the entire fabrication process. We are also currently investigating cuff electrode lengths and diameters appropriate for this upper extremity application.

Next Quarter
During the next quarter, we intend to: 1) establish a complete set of protocols for fabrication of an *entire* cuff electrode, 2) complete the validation of the fabrication process, and 3) fabricate cuff electrodes suitable for human implantation.

References
Naples, GG, Mortimer, JT, Scheiner, A, and Sweeney, JD, "A Spiral Nerve Cuff Electrode for Peripheral Nerve Stimulation", IEEE Trans. Biomed. Eng., 35:905-916, 1988.

Veraart, C, et. al., "Visual sensations produced by optic nerve stimulation using an implanted self-sizing spiral cuff electrode", Brain Res., 813:181-6, 1998.

Design of an EOG-based Command Interface for Prosthetic Control

Contract section: E.1.a.iv   Command sources for high tetraplegia

Note: The following is the abstract from a masters thesis. The full document is available upon request (Chen, Yingxi; "Design of an EOG-based Command Interface for Prosthetic Control", M.S. Thesis, Dept. of Elec. Eng. & Comp. Sci., CWRU, August 2003 *(expected date)*).

Abstract

        Using eye gaze as a control command source is an attractive option for rehabilitation robotics and neural prostheses. In this thesis, the design and implementation of an electrooculography (EOG)-based gaze-controlled robotic system is presented.

        The robot system consists of signal acquisition, pattern recognition, control strategy and robot motion modules. The user's eye gaze movements are reconstructed from EOG signals, which are recorded from the face in real time. Eye movement patterns, e.g., saccades, fixation and blinks are detected from the raw eye gaze movement data by a pattern recognition module. The control strategy module interprets the user's intention from the eye movement patterns and sends it to a robot motion-control module, which controls the robot movement according to the interpreted user intention.

        A distributed control architecture was designed to allow flexible tests and simulation of this system across an intranet/internet network. Using a dynamic binding algorithm, the major modules (or the simulation blocks of them) can be run separately in local or remote computers to enable flexible robot testing and rapid control strategy design.

        A performance metric was defined in terms of a 2-D acquisition task. Volunteers controlled the robot arm via EOG signals to direct the hand towards randomly illuminated LED targets. Target acquisition times constituted the performance metric. Experimental results for two interface designs (velocity control vs. position control) are compared. The design, implementation, and experimental results are presented in detail.

Real-time Control of Neural Prostheses

Contract section: E.1.a.vi   Implementation and Evaluation of Neuroprosthesis for High
                                        Tetraplegia

Note: The following is the abstract from a masters thesis. The full document is available upon request (Holmes, Kimberly, A.; "Real-time Control of Neural Prostheses", M.S. Thesis, Dept. of Biomed. Eng., CWRU, May 2003).

        A feasibility study of real-time control environments for the development of neural prostheses was done with two products from the Mathworks, Inc.; Simulink and xPCTarget, as well as a commercially available single board computer. The hand grasp command and control algorithm, developed at CWRU, was implemented in order to demonstrate the ability of the system. It was shown through standard benchmarks that the capabilities of the real-time control environment were not a limiting factor in the system. The real-time capabilities were quantified and shown to exceed specifications for current neural prostheses, allowing for the integration of more complex algorithms that utilize advanced control schemes, such as the use of feedback control and multi-joint movement restoration. It is thought that this approach to software and hardware development will greatly simplify and accelerate the development of control systems for a wide range of neural prostheses.

Testing of Stimulation Artifact Suppression Technique and Protocols to be Used in Percutaneous Implementation of Myoelectric Controlled Neuroprosthesis

Contract section: E.1.b   Control of Grasp Release in Lower Level Tetraplegia

Abstract

The purpose of this research is to develop and evaluate an advanced neuroprosthesis to restore hand function in persons with OCu:5 and OCu:6 (International classification) spinal cord injuries. Through this work we will implement in human subjects a control methodology utilizing myoelectric signals (MES) from muscles that can act in synergy with hand function to govern the activation of paralyzed, electrically stimulatable muscles of the forearm and hand. This work encompasses the following objectives:

1) Characterize the myoelectric signals (MES) recorded from a pair of muscles synergistic to hand function, demonstrating that the signals are suitable for neuroprosthesis control
2) Demonstrate the ability of subjects to use the proposed control algorithm to perform simulated neuroprosthesis functions and to control a virtual hand
3) Implement myoelectric control of the hand grasp neuroprosthesis in subjects with C7 level spinal cord injury and evaluate hand performance

Progress Report

During this quarter, a manuscript describing the work that focused on the first two objectives was prepared and submitted for publication to the Journal of Rehabilitation Research and Development. Also, further progress was made toward achieving the third objective stated above. Pilot experiments involving a single subject were conducted to test the adequacy of the stimulation artifact suppression technique and the protocols for customizing the control strategy and evaluating controllability. In addition, several individuals with C7 spinal cord injury have been evaluated for enrollment in this study.

Subject and Electrode Implantation

The subject in our pilot experiments was a 32-year old able-bodied student investigator on this study. Two MES recording electrodes and three stimulating electrodes were implanted in muscles of the left forearm. The subject was enrolled in the protocol for 3 weeks. No experiments were conducted until one week after electrode implantation. Experiments were then conducted over the next two weeks.

MES electrodes were implanted in the flexor carpi radialis (FCR) and in the extensor carpi radialis brevis (ECRB). Prior to implantation, the skin was numbed using a topical anesthetic (EMLA® cream), and cleansed with Betadine® and alcohol. The MES electrodes we used were constructed from pairs of stainless steel fine wire that were coiled into a lead having an outer diameter of 0.38 mm and loaded into a 22-gauge needle (see Quarterly Progress Report #7 for a picture). The MES electrodes had different spacing between the bipolar recording contacts. The electrode in the FCR had a spacing of 1 mm, and the electrode in the ECRB had a spacing of 4 mm between recording surfaces. A second MES electrode was implanted in the ECRB with a 1 mm spacing in order to study the effect of the bipolar spacing on signal

characteristics, but that electrode was removed because it had accidentally been tugged during the implant procedure and was not adequately recording MES.

Stimulating electrodes were implanted in the flexor digitorum superficialis (FDS), extensor digitorum communis (EDC), and flexor pollicis longus (FPL). Two types of stimulation electrodes were used. The FDS and EDC electrodes were manufactured from multi-stranded stainless steel wire wound into a coiled lead with an outer diameter of approximately 0.58 mm and loaded into 19-gauge needles. The FPL electrode was a monopolar straight fine-wire electrode (Nicolet Biomedical, Inc.) inserted with a 25-gauge needle. Stimulation that was delivered through the FDS electrode gave strong flexion of the ring and middle fingers, and stimulation through the EDC electrode gave strong extension of the middle finger. The electrode targeted to the FPL did not elicit thumb flexion upon stimulation, but instead recruited FCR and FDS muscles. This electrode will be referred to as the FCR/FDS electrode. These few stimulation electrodes were not sufficient to provide a functional stimulated hand grasp, but were adequate for evaluating the procedures and laboratory setup that will be used in the percutaneous studies.

Stimulation Artifact Suppression

Setup: A block diagram of the laboratory setup that was used for the artifact suppression experiments is shown in Figure 4. MES were differentially amplified by an EMG amplifier (Cambridge Electronic Design, Ltd.), which suppressed stimulation artifact by grounding the MES inputs for a programmable duration in response to a trigger signal. The trigger signal was a single pulse produced by the stimulator at a frequency of 12 Hz, the stimulation frequency. The onset of the trigger pulse

Figure 4. Block diagram of setup.

was 2 msec prior to the onset of stimulation pulses delivered to the target muscles; hence, MES blanking began slightly before stimulation was delivered to the muscles. The grounding capability of the amplifier could be turned on and off by a switch box. The amplified signals were digitized at 2500 Hz and displayed on a computer screen. In addition to the artifact suppression provided by the amplifier, a portion of the digitized MES could be zeroed or deleted digitally for a programmable duration after the onset of the blanking trigger using a custom LabView™ routine.

A grasp pattern was programmed into the stimulator for the subject. The grasp pattern mapped a single command signal value, ranging from 0 to 100, to a particular current pulse-width to be delivered by each stimulation electrode. The grasp pattern used for our subject is shown in Figure 5, where a zero command value corresponded to maximum stimulation of the EDC and no stimulation of the FDS and FCR/FDS, and a command value of 100 corresponded to no EDC stimulation and maximum stimulation of the FDS and FCR/FDS. The stimulation frequency was set at 12 Hz (an interpulse interval of 83 msec). The stimulator was interfaced with the computer so that the command signal could be modulated using software controls in LabVIEW™ (Figure 4).
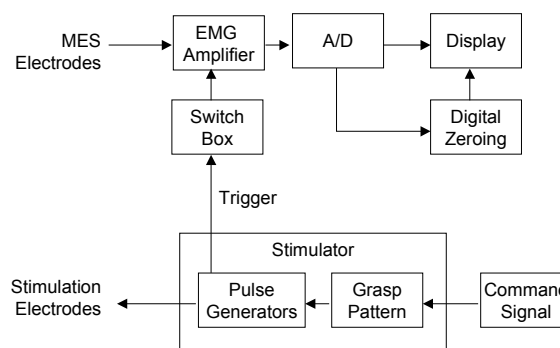
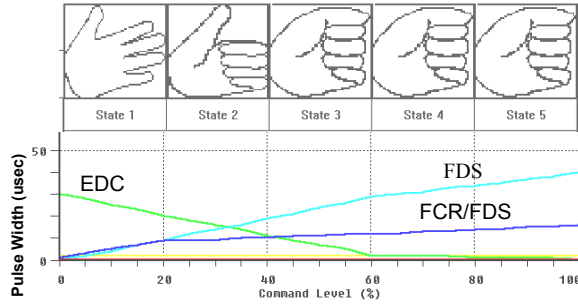*Experiment and Results*: Several trials were conducted in which the subject kept the


Figure 5. Lateral grasp pattern

wrist muscles relaxed while stimulation was turned on with and without artifact suppression on. In some trials the command signal was modulated from 0 to 100 and back to 0, causing stimulation to extend the fingers, flex the fingers, and extend the fingers again. In other trials the command signal was kept constant at 0 (finger extension) while amplifier blanking and digital zeroing were turned on and off.

As expected, the size and shape of the stimulation artifact changed as the command signal was modulated (Figure 6). When the command level was 0 (maximum EDC stimulation), the artifact was larger in amplitude and duration in the ECRB recording than in the FCR recording (Figure 6A). This was expected because the MES electrode in the ECRB was closer to the stimulation electrode in the EDC than the MES electrode in the FCR. Conversely, when the command level was 0 (maximum FDS and FCR/FDS stimulation), the artifact was larger in the FCR recording than in the ECRB recording (Figure 6B).
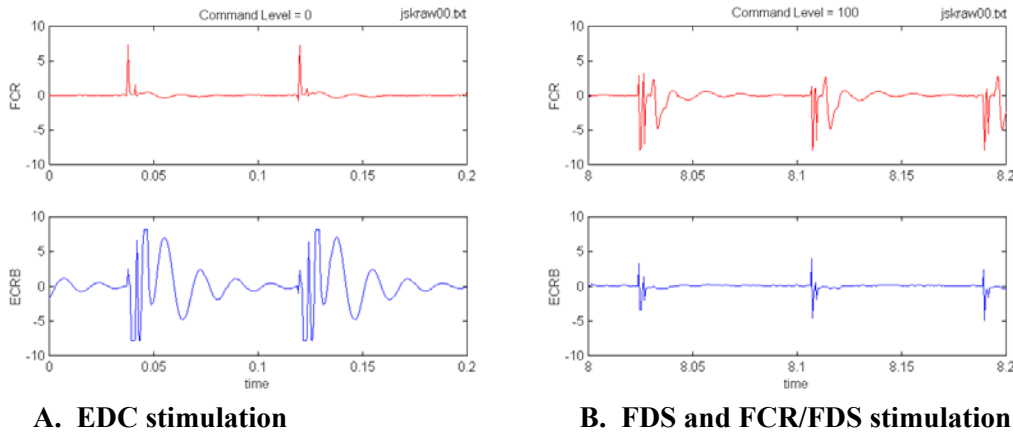
A. EDC stimulation   **B. FDS and FCR/FDS stimulation**

**Figure 6.   Stimulation artifact in the ECRB and FCR signals.   A. Command level at 0
corresponds to maximum stimulation of EDC.   B. Command level at 100
corresponds to maximum stimulation of FDS and FCR/FDS.**

The largest magnitude stimulation artifact occurred in the ECRB MES when the EDC was maximally stimulated (Figure 6A). That stimulation also appeared to elicit M-waves in the ECRB and subsequent baseline oscillations that lasted most of the entire interpulse interval. Later tests showing MES activity during finger extension suggested that the ECRB MES electrode may have been partially placed in the EDC, accounting for the M-wave observed here. Based on the size and shape of the largest stimulation artifact, the grounding period of the amplifier was adjusted to the largest available duration, 42 msec. In addition, digital zeroing was
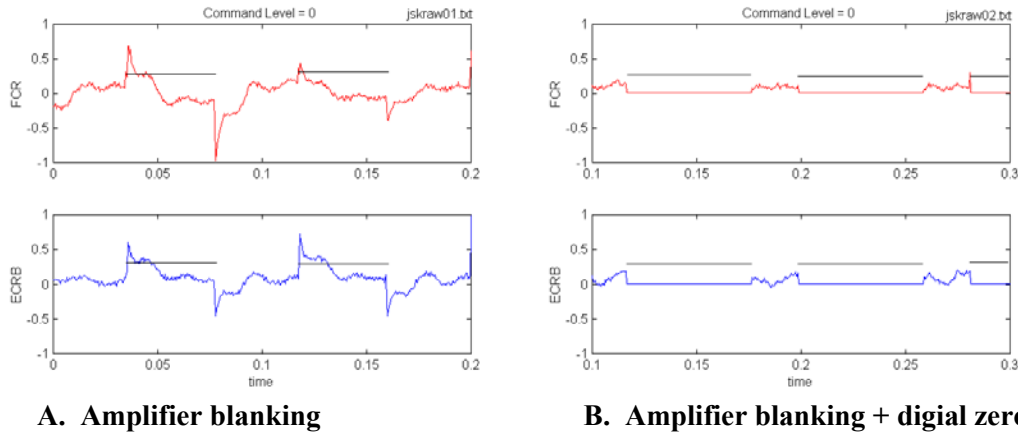
A. Amplifier blanking   **B. Amplifier blanking + digial zeroing**

Figure 7.   Effectiveness of artifact suppression.   Wrist muscles were relaxed, and EDC was being stimulated at 12 Hz.   A. The amplifier grounding duration, indicated by the black bars, was set to 42 msec.   B.   Amplifier grounding (42 msec) and digital zeroing for 60 msec, indicated by the black bars, was used.

employed, where the zeroing period used was set to 60 msec, leaving 23 msec of MES every interpulse interval to be used for control.

The grounding provided by the amplifier effectively prevented stimulation artifact from being recorded, but added noise to the signal at the onset and offset of the grounding period (Figure 7A). When digital zeroing was added, the noise produced by the amplifier was also removed from the signal (Figure 7B) leaving a signal showing only baseline myoelectric activity in the muscles. Therefore, amplifier blanking coupled with digital zeroing or deletion appears to provide adequate stimulation artifact suppression.

Customizing the Control Strategy

Setup: The setup for these experiments is similar to that shown in Figure 4, except that instead of digitally zeroing the signal, the blanked portion of the MES was deleted and the remaining 23 msec of MES per interpulse interval was smoothed for use as a control signal. The digital processing included rectification and smoothing using a running time window averager with a window length of 250 msec that updated every 83 msec (interpulse interval). The processed signal was displayed in real-time on the computer screen.

Experiments and Results: Our purpose was to establish a procedure for customizing the control strategy. This required the collection of MES during wrist relaxation and sustained wrist flexion and extension contractions. The procedure we used was generally the same as what was done in previous experiments in which no stimulation was being used (see Quarterly Progress Report #5). That procedure involved recording baseline activity while moving the arm to different postures with and without a weight fastened to the hand, and recording MES during sustained wrist flexion and extension while the arm was held at different postures with and without a weight fastened to the hand. The resulting MES patterns were used to determine the placement of decision boundaries, which define the control strategy. The same procedure was followed except that electrical stimulation was used in place of a weight on the hand. All the trials were repeated three times – first with no stimulation, then with stimulation on at a command level of 0, then with stimulation on at a command level of 100.

10

Figure 8 shows the results of a target tracking task performed without any stimulation or blanking and with EDC stimulation at a command level of 0 with blanking. The stimulation and/or blanking did not prevent the subject from being able to perform the tracking task well, but did increase the noise (ripple) in the signal, about two-fold.
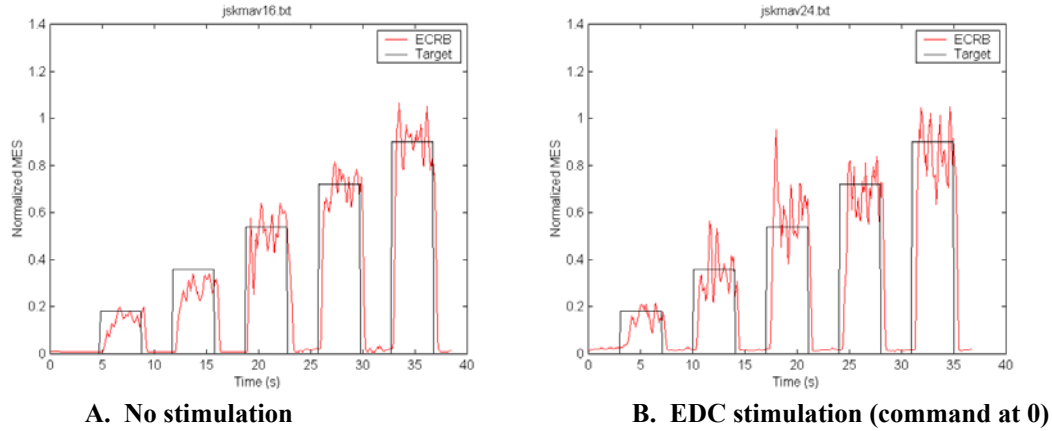

A. No stimulation   **B. EDC stimulation (command at 0)**

Figure 8. Sustained wrist extension contractions. Stimulation increases noise in the MES.

Figure 9 shows the MES data acquired during sustained wrist flexion and extension across all the trials. This subject was able to perform isolated contractions of the wrist muscles. Electrical stimulation of finger flexors and extensors during wrist flexion and extension did not hinder the subject from being able to produce isolated FCR and ECRB contractions of various strengths.

Figure 9. MES pattern produced during sustained wrist flexion and extension. Boundaries were placed to define the Open, Close, and Hold neuroprosthesis states.

Testing Controllability

Setup: The control algorithm represented in Figure 9 was added to the setup after the MES processing stage. The control algorithm updated the command signal every interpulse interval (83 msec). Therefore, the command signal was not modulated by the manual control, but according to the MES and the control algorithm.

Experiments and Results: The state activation test and position matching tests, as described in previous progress reports (see Quarterly Progress Report #6), were conducted with the arm held in front of the subject, the forearm neutral, and stimulation to the muscles modulated by the control algorithm. The state activation test required the subject to activate the Open, Close, and Hold neuroprosthesis states in response to a target cue. The position matching test required the subject to control the opening and closing of the needles on a dial (virtual hand) and attempt to match target positions superimposed on the dial. The results of these two tracking
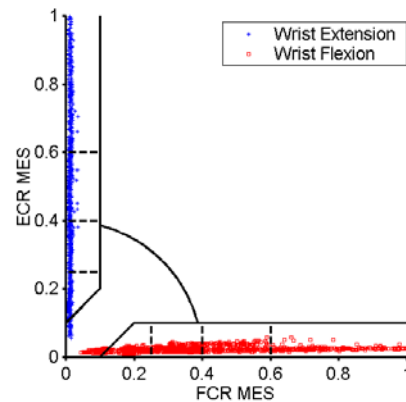
tests are shown in Figure 10. The success rate in activating the target state was 100%, and the percentage of target presentations during which an inadvertent state was activated was 17.5%. The average duration of an inadvertent state activation was 148 msec. The results of the position matching test were perfect – 100% success in matching within +/-5% the target position and no inadvertent changes in hand position.

In future experiments that will be performed with C7-injured participants, an adequate number of stimulation electrodes will be implanted to provide the subject with a functional hand
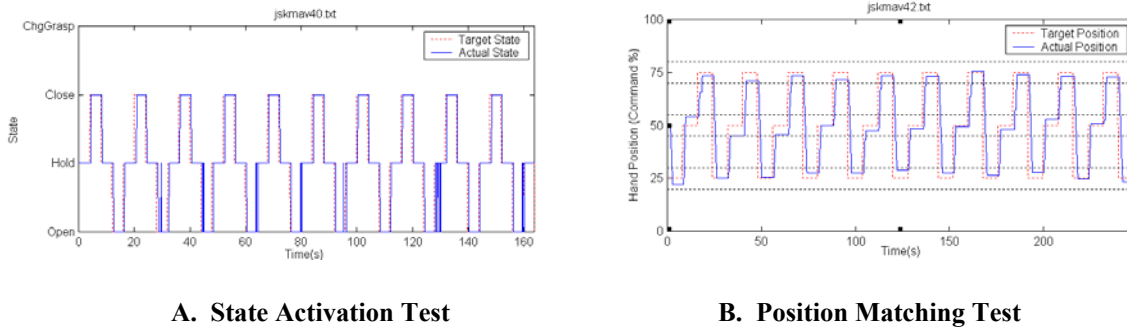

A. State Activation Test	B. Position Matching Test

Figure 10. Target tracking tests of controllability.

grasp. In addition to the state activation and position matching tests, tests will be conducted to evaluate the subjects' ability to perform tasks with their stimulated hand under myoelectric control.

Conclusions

An artifact-free MES can be obtained by using an EMG amplifier that grounds the inputs during the stimulation artifact, and by deleting the portion of the MES that overlaps the grounding period. The protocols for collecting MES data that are required for the control strategy customization and for preliminarily evaluating the subject's ability to use MES control have been established. Greater care in checking the placement of recording and stimulation electrodes during the implant procedure will be exercised to ensure that the electrodes are recruiting or recording from the desired muscles. Shorter and smaller-diameter needles for implanting the stimulating electrodes will be less unwieldy and make the procedure more tolerable for the patient.

Next Quarter

A subject with C7 spinal cord injury will be recruited to participate in the part of this work that involves percutaneous implementation of the neuroprosthesis. We will establish appropriate artifact blanking parameters for the subject, customize the control algorithm to the subject's MES, test the subject's ability to perform simulated neuroprosthesis functions and actual hand grasp tasks. We will compare their ability to use myoelectric control with a controller in which the command signal is proportionally modulated by use of a wrist-angle sensor.

An Integrated Voluntary Muscle and FES Controller to Restore Elbow Extension in Spinal Cord Injury

Contract section: E.2.a.ii.4.1   EMG-based shoulder and elbow controller

Introduction

The objective of this research is to develop and assess a synergistic controller employing voluntary elbow flexor and shoulder electromyograms (EMG) to control stimulated elbow extension in individuals with C5/C6 spinal cord injury (SCI). The control system utilizes natural synergies, integrating remaining voluntary control with functional electrical stimulation (FES) to the paralyzed triceps. The controller should provide synergistic triceps stimulation requiring little to no subject training. In other words, the subject should simply attempt to move their hand to a specific location or apply an endpoint force at the hand and the controller should apply the appropriate level of triceps stimulation (Figure 11). Endpoint force vectors at the hand are a function of, among other factors, the moment generated at the elbow joint. The extension moment generated about the elbow joint is a function of the triceps muscle activation. Some shoulder and elbow flexor muscles are usually under some degree of voluntary control in C5/C6 SCI. We hypothesized that the remaining voluntarily controlled upper extremity muscles produce a repeatable, recognizable pattern of EMG signals indicative of the level of triceps stimulation needed for the desired position and endpoint force of the arm. In order to test this hypothesis, EMG from voluntary elbow flexor and shoulder muscles will be used as inputs to train and test an artificial neural network (ANN) to output triceps stimulation level. The hypothesis will be accepted if the trained ANN converges to a solution that yields low error when both training and generalization data are applied, the controller relationships are indicative of those predicted by a biomechanical model, and the output characteristics of the controller are stable.
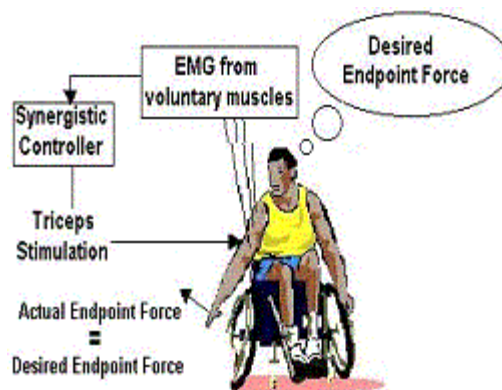

Figure 11. **The controller should let an SCI subject move their arm or apply an endpoint force simply by attempting to do so.**

Methods

A biomechanical model of the shoulder and arm was used to determine estimates for the elbow extension moment needed to achieve isometric endpoint force vectors of different magnitudes and directions at three locations in a subject's workspace (Figure 12). Next, recruitment curves of triceps stimulation versus elbow moment were measured to determine stimulus levels required to generate the elbow moments predicted by the model. A PC-based lab system was interfaced to the neuroprosthesis external control unit of a
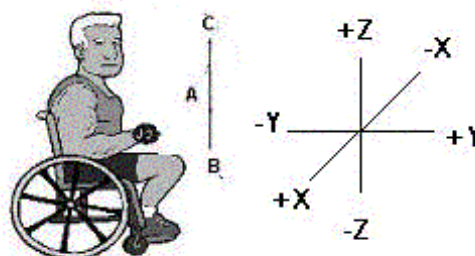

Figure 12. **Data was collected at a variety of endpoint locations shown above. The axis is also shown.**

C5/C6 SCI subject and used to control triceps stimulation. Using the lab system, EMG signals from voluntary elbow flexor and shoulder muscles were collected while the subject generated isometric endpoint force vectors of different magnitude and direction using stimulation levels predicted by the model and recruitment curves. The collected data was used to train and test an ANN to output triceps stimulation using EMG's as inputs.

A. Subject Description

All subjects participating had complete C5/C6 spinal cord injuries and had been previously implanted with an FES hand grasp system including an implanted triceps electrode. All subjects had a paralyzed triceps and a few to several proximal arm muscles left under voluntary control including elbow flexor and shoulder muscles (Table 1). The synergistic controller should be applicable to subjects whose number and strength of voluntarily controlled muscles differ since a separate network will be trained for each subject. For subject 1 the left arm was evaluated.

Muscle	Abbrev.	Chief Action	Subject 1
Biceps	BI	Flexion and supination of forearm	X
Brachioradialis	BR	Flexion of forearm	X
Upper Trapezius	UT	Elevation of the scapula	X
Middle Trapezius	MT	Retraction of the scapula	X
Lower Trapezius	LT	Depression of scapula	X
Anterior Deltoid	AD	Flexion of the arm	X
Middle Deltoid	MD	Abduction of the arm	X
Posterior Deltoid	PD	Lateral shoulder rotation, arm extension	X

Table 1. Subjects who have sustained a SCI at the C5/C6 level may have several muscles that remain under voluntary control. The table above illustrates a possible set of these muscles and also the exact muscles that were recorded from in each SCI subject.

B. Biomechanical model of the shoulder and arm

A biomechanical model of the shoulder and arm was used to obtain estimates for the magnitude of elbow extension required for a subject to generate force vectors of varying magnitudes and directions. The controller should allow subjects to generate and control endpoint force vectors unachievable without triceps stimulation. To accomplish this, the neural network needed to be trained with EMG data collected while the subject generated endpoint force vectors both inside and outside of their voluntary range. Achieving force vectors outside of their voluntary range requires triceps stimulation. Additionally, once trained, the network will operate during triceps stimulation. These requirements created a dilemma. An ANN that needed training to output an appropriate level of triceps stimulation needed to be trained with EMG data collected during the appropriate level of triceps stimulation. Therefore, a reasonable stimulation level estimate for each goal vector to be attempted by each subject during data collection was needed to work around the dilemma.

A biomechanical model was used to estimate the force and moment contribution of individual proximal arm muscles based on kinematic and kinetic inputs. Specifically, we specified the external forces and arm geometry, and the model predicted the elbow extension moment required by the triceps. This model used a finite element method to determine muscle activations for given inputs including the orientation of the arm and

external forces acting on the hand. The optimization criterion minimized the squared sum of the muscle stresses (muscle force/physiological cross sectional area of the muscle). Arm geometry was defined for each data collection end point position such that the elbow pointed down. This minimized subject discomfort and shoulder muscle fatigue. This model allowed the input specifications of voluntarily controlled muscles and their strengths. We tailored the model for each subject to give us subject specific outputs based on their specific remaining voluntary muscle set (Table 1). The model allowed a user-defined force generating value for each muscle ranging from 0-1. A value of 1 indicated a normal, voluntarily controlled muscle, while 0 represented a completely paralyzed muscle. Muscles that were weakened, but not completely paralyzed, were assigned intermediate values depending upon their manual muscle test scores. The exception to the above assignments was the triceps. It was considered near normal in all subjects since FES would be used to restore its ability to generate forces. By defining triceps as near normal in the model, we obtained the elbow extension moment produced by triceps that was needed to achieve the desired endpoint force.

Model simulations calculated the elbow extension moment required by triceps for a specific subject for each goal isometric endpoint force vector (endpoint location, direction, and magnitude) that the subject would encounter during data collection. Simulations were run at a total of three endpoint locations (Figure 12). At each location forces were applied along both the positive and negative directions of the x, y, and z-axes in steps of 10 N, ranging from 0 – 70 N. Moment tables were then created and stored for each subject that contained the elbow extension moment required by triceps to produce goal force vectors of different magnitude, direction, and endpoint location.

C. Elbow Extension Moment Recruitment Curves

Experimentally measured elbow extension recruitment curves were used to calculate stimulation estimates for data collection. The biomechanical model yielded elbow extension moments required by triceps for particular subjects, arm kinematics, and endpoint forces. However, we needed to know a reasonable level of triceps stimulation to apply. For each subject, we experimentally measured elbow moment as a function of stimulus level (recruitment curve). Recruitment curves for elbow extension moment versus triceps stimulation level were collected using an elbow moment transducer [Memberg, 2001]. The stimulation pulse width was increased from 0 μs to 200 μs in steps of 20 μs. The stimulation pulse width was then decreased from 200 μs to 0 μs in steps of 20 μs. Obtaining recruitment curves in both increasing and decreasing directions of stimulation allowed compensation for hysteresis. Data was collected for various arm orientations that matched anticipated data collection positions. A 5th order polynomial was then fit to scatter plots of elbow extension moment versus stimulation pulse width to create the inverse recruitment curves. The values in the elbow extension moment table yielded by the biomechanical model for a particular subject were then used to create a table of triceps stimulation levels using the inverse recruitment curve equation (Figure 13). The table of stimulation levels for a particular subject was then stored and used later during data collection. The minimum allowable stimulation pulse width was 0 μs and the maximum was 200 μs. The biomechanical model also predicted when a certain level of force was not achievable with the remaining voluntary muscle set of the subject. If the model indicated that goal forces previous to this "not achievable" value required an increasing level of

triceps elbow extension moment, then the stimulation was set to 200 µs in these instances, and the trial for that goal vector was still attempted during data collection.
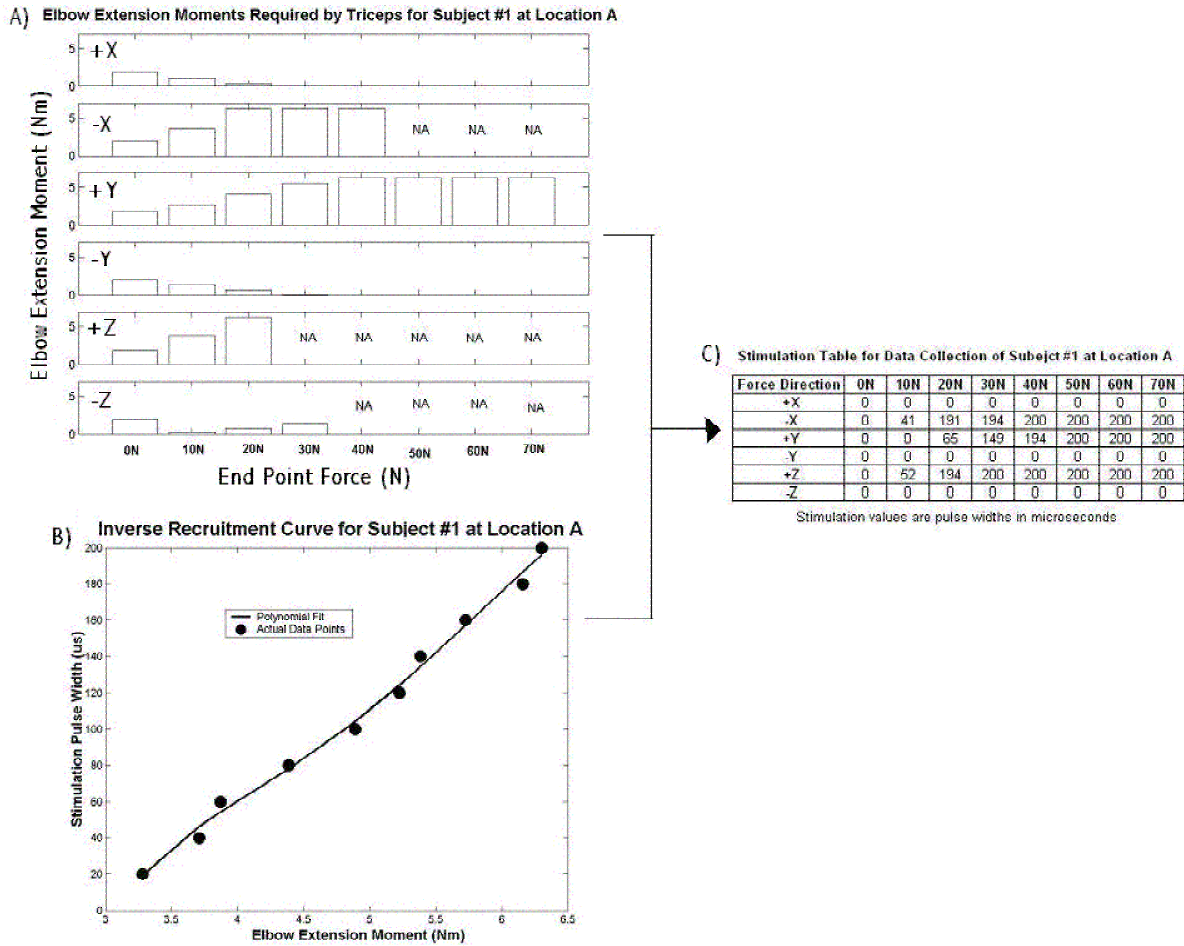

Figure 13. A) A biomechanical model of the shoulder and arm were used to determine the elbow extension moments required by triceps to generate forces along each of three axes from 0 to 70 N in steps of 10 N. An example of required elbow extension moments for subject 1 at location A are plotted as a function of increasing endpoint force. Plots are shown for both the positive and negative directions of each axis. NA indicates that the model predicted a subject could not reach that endpoint force regardless of the amount of triceps elbow extension moment based on their remaining set of voluntary muscles. B) An inverse recruitment curve was plotted for subject 1 at location A. Stimulation is plotted as a function of elbow extension moment. A polynomial was fit to the data points and also plotted. C) The elbow extension moments predicted by the model were plugged into the polynomial fit equation to calculate a table of stimulation pulse widths to use for subject 1 at location A during data collection.

The recruitment curves were also used to determine the maximum allowable error that the controller could produce. One criterion for accepting our hypothesis is that the error in the system must be low when both the training and generalization sets are applied to the trained network. Error was related to anticipated function using elbow moment. We limited the allowable elbow moment error to 25% for each subject. We used the inverse recruitment curves to determine the smallest difference in pulse widths that produces a

25% difference in elbow moment. This value will be the maximum mean squared error (MSE) error in pulse width allowed.

D. Data Collection and Signal Processing

Surface EMG was collected from C5/C6 SCI subjects' voluntarily controlled elbow flexor and shoulder muscles (Table 1) while they attempted to match goal isometric endpoint force vectors at a variety of endpoint locations (Figure 12). These endpoint locations were chosen to simulate an area where subjects would perform weight shifts or transfers (B), an area for manipulating objects (A), and an area for overhead reach (C). Subjects donned a small cast to stabilize their wrist joint. A gimbal interfaced the cast to a JR3 force and moment transducer. The gimbal reduced pure moments generated by the subject. A visual 3-D display on a computer monitor provided magnitude and direction feedback of the goal and subject generated force vectors. Subjects tracked goal force vectors along each axis at each location (Figure 14). The subject attempted to track the goal force along the specific axis and maintain forces in the other two axes as close to zero as possible. The goal vector started at 0 N and then increased in 10 N increments along the positive direction of the axis each time the subject maintained the current goal for a few seconds. This continued until the subject could not generate any larger force. The procedure was then repeated along the negative direction of the same axis. During each data collection session, data was collected twice for each axis at each location. The order of the axes was randomized, however, all data collection occurred at one location before moving on to another to reduce overall test time and minimize subject discomfort.

In addition to tracking in 10 N increments along an axis, tracking was also completed over smaller regions where the predicted stimulation changed most quickly. For example, the stimulation levels predicted by the model and inverse recruitment curves for subject 1 can be seen in Figure 13c. For the negative x direction, the stimulation changed most rapidly between 10 N and 20 N (41 to 191 μs). The neural network controller needed training with a large range of stimulation output pulse widths to ensure good generalization over all regions of the output space. Therefore, to provide a rich output training set for the neural network, the subject also tracked forces that ranged from 10 N to 20 N in steps of 2 N in this region. The stimulation pulse widths for this area were computed as described above. Similar procedures were used for other subjects and areas of quickly changing predicted stimulation levels to ensure a rich training set.

During data collection stimulation was delivered to the triceps at 20 mA, 12 Hz, with a variable pulse width from the subject specific stimulation table. Since stimulation was delivered to the triceps at 12 Hz (every 83 ms), all EMG channels were sampled at 2500 Hz for 80 ms using a data acquisition (DAQ) system from National Instruments, Austin, TX. Blanking EMG amplifiers (1902 Programmable Signal Conditioner, Cambridge Electronic Design Limited, Cambridge, U.K.) were used to remove the stimulus artifact from the EMG signals. For each channel of EMG, software (LabVIEW 5.0.1, National Instruments, Austin, TX) calculated the RMS value of the EMG segment between each stimulating pulse and normalized it to the maximum and minimum RMS EMG segment for that muscle (Figure 14). The discrete time RMS EMG values were then filtered by an adaptive, step-size filter. The processed and filtered EMG command signals were used as inputs to train the neural network.
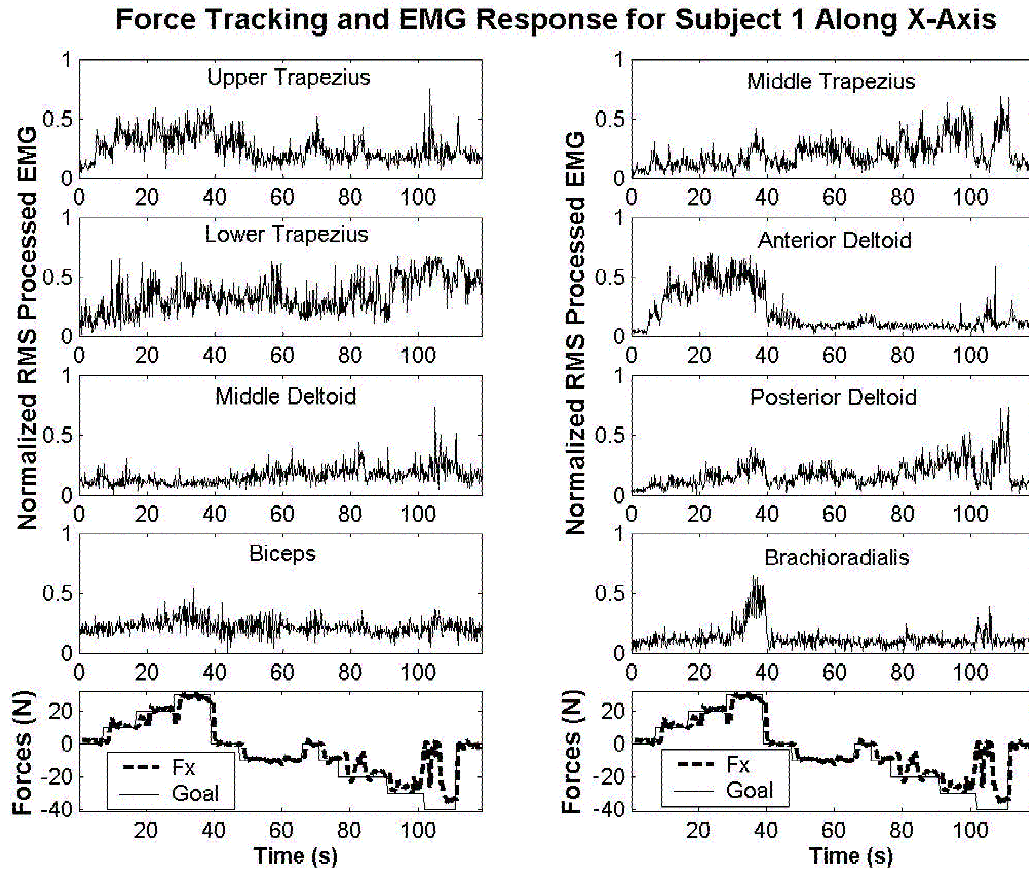
Figure 14. During data collection subjects tracked goal isometric force vectors. Illustrated above are subject 1 tracking force vectors along the X-axis. Also plotted are the RMS processed EMG signals during this data collection. The force plots are both the same, presented below the EMGs for easy comparison.

E. Neural Network Training

Our objective was to train the network to recognize arm endpoint intention of a subject and allow subjects to make movements and create forces that are in part controlled by the output of the neural network. The EMG command signals (inputs) and triceps stimulation levels (outputs) used during data collection were used to train a neural network. The neural network was trained with a subset of all collected data for a particular subject known as the valid data set. The valid data set included data with an acceptable tolerance of generated endpoint force as compared to the goal endpoint force. For all data collection tracking trials that were performed in increments of 10 N, valid data was accepted if the force in the tracking direction was +/- 5 N of the goal and the forces in the other two directions were less than 10 N in magnitude. For tracking trials that were completed in 2 N increments, valid data was accepted if the force in the tracking direction was +/- 1 N of the goal and forces in the other two directions were less than 5 N in magnitude.

The valid data set was further randomly separated into a training set and a generalization set. The training set consisted of 90% of the valid data set with the generalization set comprising the other 10%. To ensure that the network was trained with

an equal amount of data from each location and axis, the training and generalization sets were first taken from the valid data set from each collected data trial along an axis. These sets were then combined into one training and one generalization set.

After a training set was created for a particular subject, the MATLAB Neural Network Toolbox (MathWorks Inc, Natick, MA) was used to train a neural network. The inputs to the network included the voluntary EMG command signals, and the output was the triceps stimulation level (taken from the stimulation table for that subject) used to obtain the goal force vector at that time. The two-layer network structure consisted of one hidden layer with five neurons and an output layer with "tansig" transfer functions used at each hidden layer node. The network was trained offline using resilient backpropagation batch training. All inputs and outputs to the network were normalized to the range 0-1. The initial weights and biases of the network were randomly selected. Networks were trained and tested separately for each subject. We trained the neural network structure three times each using every possible combination (255 possible combinations) of muscle inputs. Using fewer electrodes to record EMG would simplify the eventual clinical implementation. For example, during data collection for subject 1 we recorded eight channels of EMG. A practical implanted system would ideally have only 2 or 3 implanted EMG electrodes.

F. Synergistic Controller Verification

After training, the neural network controller was evaluated to determine if it was working properly. First, we verified that the error produced was within an acceptable tolerance. To verify an acceptable error when the training set was applied, we applied the training set to the trained network and calculated the MSE. This was completed each time a network was trained. To verify an acceptable error when the generalization set was applied, we applied the generalization set to the trained network and calculated the MSE.

We also qualitatively evaluated if the trained network controller was working as predicted by the relationships of the biomechanical model. The stimulation levels predicted by the model increased or decreased as the force along a specific axis and direction increased. These relationships were evaluated by simulating the trained neural network controller. The continuous-time EMG data collected for a particular subject as they tracked along an axis during data collection was used to simulate the network running in real-time. Using EMG inputs from collected data trials, we calculated the output of the controller. The controller output was filtered by an adaptive step-size filter.

Results/Discussion

A. Biomechanical Model and Predicted Stimulation Table

The biomechanical model yielded reasonable estimates of the triceps extension moment that should be applied for a given goal force vector. The elbow extension moment needed was a function of the subject's voluntary set of muscles, arm kinematics, and endpoint forces. The model predicted the extension moment for both the lateral and medial heads of the triceps. These muscles act in parallel to extend the elbow joint. Therefore, these moments were added together to calculate the elbow moment prediction. The biomechanical model predicted relationships for increasing or decreasing stimulation along

a specific axis and direction for a particular subject. For example, consider the left arm of subject 1. The model predicted that the elbow extension moment due to triceps should increase in the -x, +y, and +z directions (Figure 13, A). The model predicted elbow extension decreases to zero as force increases in the other directions.

Recruitment curves were measured with both an increasing and decreasing level of stimulation. This yielded a difference in recruitment curves due to hysteresis. This was compensated for by taking the average of the data points between the two curves and creating a new recruitment curve based on these points (Figure 13, B). A 5th order polynomial equation was computed to fit these points. The extension moments predicted by the model were used as inputs to this equation to generate a table of stimulation values for use during data collection (Figure 13, C). The stimulation table for subject 1 illustrated that stimulation was required in force directions that required elbow extension while it was zero for force directions that did not require elbow extension. Also, for subject 1 the recruitment curves predicted that the smallest difference in pulse widths that produced a 25% change in elbow extension moment was 40 μs or 0.2 normalized. Therefore, the minimum allowable MSE for subject 1 was 0.04.

The biomechanical model of the shoulder and arm produced reasonable estimates of elbow extension moments required for C5/C6 SCI subjects to generate isometric endpoint force vectors at various locations. The stimulation estimates calculated using the model and inverse recruitment curves allowed subjects to successfully track isometric endpoint force vectors during data collection. While more aggressive levels of stimulation during data collection may have also allowed subjects to achieve these force vectors, this level of stimulation allowed users to naturally control their remaining voluntary muscle set. In other words, they should not need to adjust the activations of their voluntary muscle set to compensate for the triceps stimulation. Rather, they should simply activate their remaining muscle set in a natural way while it is complemented by an appropriate level of stimulation to achieve the endpoint force. This not only provides a natural control method for subjects to learn with minimal training, but should also limit fatigue in both the triceps and voluntarily controller muscles during system operation.

B. EMG Patterns in the Valid Data Set

Repeatable EMG patterns were found for subject 1 over trials along the same axis while different and recognizable patterns of EMG were found for subject 1 over trials along different axes (Figures 15 and 16). EMG was collected for each subject as they generated isometric endpoint force vectors at various locations using the stimulation levels predicted by the model and inverse recruitment curves. The collected data was then separated into a valid data set that represented when the subjects were within a specified tolerance of the goal vector during tracking. The average EMG values for the valid data set of subject 1 can be seen in Figures 15 and 16 illustrating how each EMG signal changes as a function of axis, direction, and magnitude of the force vector.

Repeatable and recognizable patterns of EMG were evident for each subject. The underlying hypothesis of this study was that repeatable, recognizable patterns of EMG should exist as a subject attempts to generate isometric endpoint force vectors of varying magnitude and direction. These EMG patterns allowed a neural network controller to be successfully trained. Patterns of EMG were initially illustrated during data collection. For example, Figure 14 illustrates patterns of EMG in subject 1 as endpoint forces were tracked

20

along the x-axis. As the subject tracked in the negative x direction, EMG increased for AD and BR. In the positive x direction, EMG increased in MT, MD, and PD. Other muscles such as BI, UT, and LT did not follow a pattern during tracking on the x-axis.
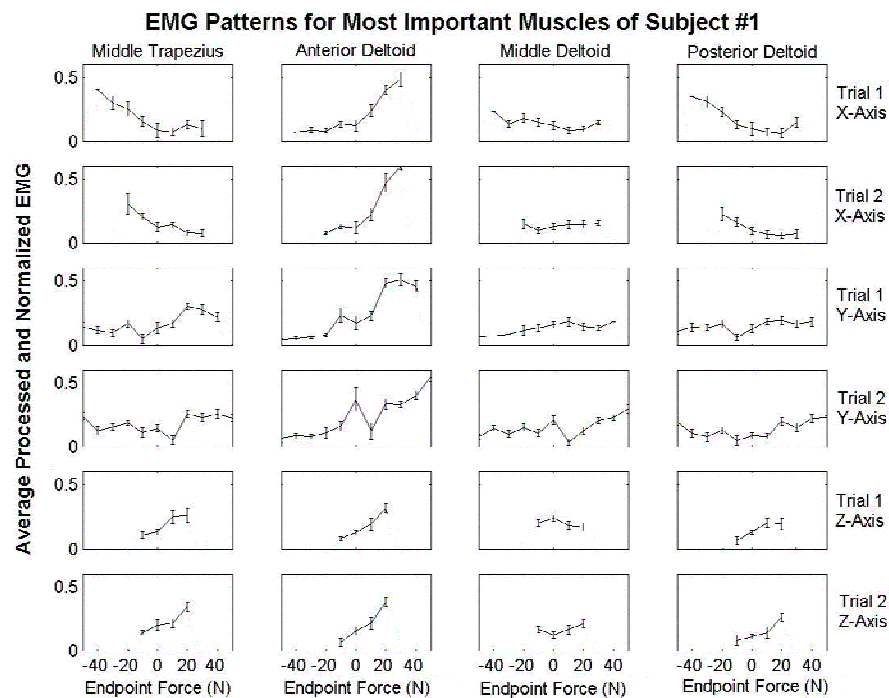

Figure 15. Patterns of EMG are illustrated for the four most important muscles of subject 1. The average EMG values from the valid data set for each endpoint force generated by the subject are shown over each axis. Two trials were completed over each axis.
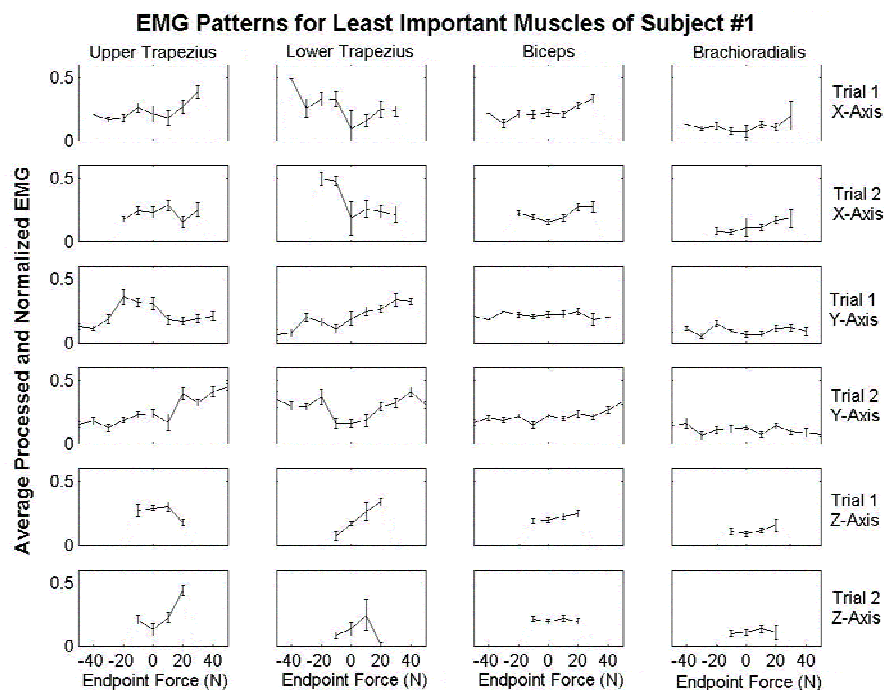

Figure 16. Patterns of EMG are illustrated for the four least important muscles of subject 1. The average EMG values from the valid data set for each endpoint force generated by the subject are shown over each axis. Two trials were completed over each axis.

21

EMG patterns were further revealed when the collected data was reduced to the valid data set. Figures 15 and 16 illustrate the valid data set for subject 1. Two trials from each axis are plotted to illustrate repeatable EMG patterns while trials from all three axes are included to illustrate recognizable EMG patterns. For example, in both trials along the x-axis AD increases as a function of increasing force in the positive x direction and decreases in the negative direction (Figure 15). Additionally, it can be seen in both trials along the x-axis that MT increases as a function of increasing force in the negative x direction and decreases in the positive direction. Similar repeatable relationships can be seen for other muscles along the same axis. A small range of EMG for a particular muscle and endpoint force vector also ensures repeatability. The small standard deviation that exists for most points verifies this repeatability. There are a few instances in which patterns do not exist or are not repeatable, such as UT during tracking of the z-axis (Figure 16). Trials 1 and 2 show different patterns of activation along the z-axis for UT. During training, the neural network recognizes that the patterns of this muscle are not repeatable and it does not provide important information for the controller.

In addition to several EMG patterns being repeatable along the same axis, EMG patterns were recognizable from one another along different axes. For example in Figure 15, during tracking along the x-axis MT shows a decreasing trend while AD shows an increasing trend. However, when tracking along the z-axis, the AD maintains an increasing trend, while MT increases. Relationships between muscle activation patterns are distinct and recognizable for particular axes. This is important since different stimulation relationships are required for different directions and axes. Muscles with repeatable patterns and more pronounced slopes typically became more important controller inputs (Figure 15) while other muscles were not (Figure 16).

C. ANN Controller Training and Verification

ANN's were successfully trained to output triceps stimulation using EMG input signals from proximal arm muscles in C5/C6 SCI subjects. Table 2 illustrates the lowest two average MSE values produced by the trained ANN for each number of muscles inputs used when the training set was applied. For example, it illustrates the two lowest average MSE values for training with only 1 muscle, the two lowest for training with 2 muscles, and so on. This list is arranged in order from the lowest error to the highest error. Certain muscles proved more important than others to the network. For example, the most important muscles for subject 1 included the middle trapezius (MT), the anterior deltoid (AD), the middle deltoid (MD), and the posterior deltoid (PD). The least important muscles for subject 1 included the upper trapezius (UT), the lower trapezius (LT), the biceps (BI), and the brachioradialis (BR). In general, using a greater number of EMG inputs produced a lower MSE.

Many of the muscle set MSE's were within our minimum allowable error (Table 2). All of these networks also produced an acceptable error when the generalization set was applied. Therefore, other criteria were developed to examine this subset of trained networks. One criterion was to use the muscle set that contained the fewest number of muscle inputs. For example, for subject 1 the smallest number of muscles used in a training set that still provided an acceptable error was three. These sets included [AD, MD, PD] and [MT, AD, MD]. Therefore, our goal was achieved in keeping the maximum elbow extension moment error to below 25% using only three muscle inputs.

Average MSE	Muscles in Set							
0.01816		MT	LT	AD	MD	PD	BI	BR
0.01831	UT	MT	LT	AD	MD	PD	BI	BR
0.01900	UT	MT	LT	AD	MD	PD		BR
0.02176		MT	LT	AD	MD	PD		BR
0.02185		MT		AD	MD		BI	BR
0.02193	UT	MT		AD	MD	PD		BR
0.02263				AD	MD	PD	BI	BR
0.02589		MT		AD	MD	PD		
0.02594		MT		AD	MD			BR
0.03230				AD	MD	PD		
0.03448		MT		AD	MD			
0.04693		MT				PD		
0.05340					MD	PD		
0.06681						PD		
0.06756		MT						

Table 2. The average MSE when the training set was applied to the trained network using the muscle set shown to the right. The network was trained a total of three times using that muscle set as an input and the average is shown.

The best muscle set to use for subject 1 was [MT, AD, MD]. This was found by qualitatively examining the expected relationship between endpoint force direction and stimulation output during controller simulations (Figure 17). The controller trained with [MT, AD, MD] output a proportionally increasing level of stimulation as the subject generated forces in the –x, +y, and +z directions, and little to no stimulation in the other directions, as predicted by the model and inverse recruitment curves (Figure 17, A, B, C). Using the muscle set [AD, MD, PD] did not allow the proper relationship to occur on the z-axis (Figure 17, E). Tradeoffs existed between using a smaller number of muscle inputs and the noise that occurred in the controller output (Figure 17, A, D, F).

A minimum of three input muscles for subject 1 could be used to train a neural network and achieve the desired MSE for both training and generalization sets. Limiting the number of muscles used will simplify the eventual clinical implementation of the controller. The neural network structure was trained three times each using every possible combination of muscles. The first criterion for successfully training the network was producing an MSE below 0.40 for both the training and generalization sets. This would ensure that the error in elbow extension moment would not be greater than 25%. The required MSE values were achieved for many muscles sets (Table 2) with the minimum number of muscles allowed being three. MSE values for generalization sets were not significantly different than those for training sets.

Table 2 also illustrates which muscles provided the most important information to the neural network and which muscles provided redundant information. In general, the muscles that provide the most important information to the network are contained in the most number of muscle sets shown. The more important muscles tend to have steeper and more repeatable slopes in their recruitment during data collection. The four most important muscles for subject 1 include MT, AD, MD, and PD (Figure 15) while the least important muscles includes UT, LT, BI, and BR (Figure 16). For example, AD is listed very frequently in Table 2 and also has one of the steepest and repeatable slopes for all axes. In contrast, UT is only contained in three sets in Table 2 and does not have a very steep slope nor is it repeatable. Redundant muscle information is illustrated by the two sets of three

23

muscles that produced the lowest MSE included [MT, AD, MD] and [AD, MD, PD]. MT and PD are the only difference between the two sets and their MSE values are extremely close. Therefore, it is possible that MT and PD provide redundant information. These two muscles have very similar shapes along each axis (Figure 15), further illustrating the redundancy. Finally, an interesting note is that PD appears to be a very important muscle. If only one muscle was used to train the network, this muscle provided the lowest MSE.

In order to further evaluate which set of three muscles would better suit the controller for subject 1, the relationships between the predicted directions requiring stimulation and simulated results of the controller were examined. The model predicted that a proportional increase in stimulation would be required as subject 1 generated force vectors in the –x, +y, and +z directions. Proportionally applying stimulation in these directions should increase the force that a subject can generate in these directions. Therefore, trained neural network controllers were simulated with data collected during tracking trials (Figure 17). The controller using the muscle set [MT, AD, MD] effectively produced an appropriate level of stimulation when the subject generated forces in all directions (Figures 17 A, B, and C). As subject 1 generated forces in the positive x direction, very little stimulation was output by the controller, but when forces were applied in the negative x direction, the stimulation proportionally increased. This verifies that the relationship predicted by the model and the trained network controller outputs are in agreement. These relationships are also true for set [MT, AD, MD] along the y and z-axes. When subject 1 is relaxed in Figure 17 C, the baseline force is not 0 for the z-axis since the weight of their arm is creating a force in the negative z direction.

The network trained for [AD, MD, PD] produced similar or slightly better results along the x and y axes (not shown), however, failed to exhibit the correct relationship along the z-axis. While the controller trained with [MT, AD, MD] (Figure 17 C) illustrates that as the subject attempts to increase their force in the positive z direction, the controller appropriately applies stimulation, the controller trained with [AD, MD, PD] (Figure 17 E) illustrates that this relationship was not learned by the controller. Therefore, we qualitatively assessed from these plots that set [MT, AD, MD] was the best set to use for subject 1. Additional simulations were conducted to illustrate tradeoffs between system error and the number of EMG channels used. Simulations were conducted over the x-axis using sets of three [MT, AD, MD], four [MT, AD, MD, PD], and two [MD, PD] muscles (Figures 17 B, D, F). In general, increasing the number of muscles inputs used improved the noise since more information was provided to the network.
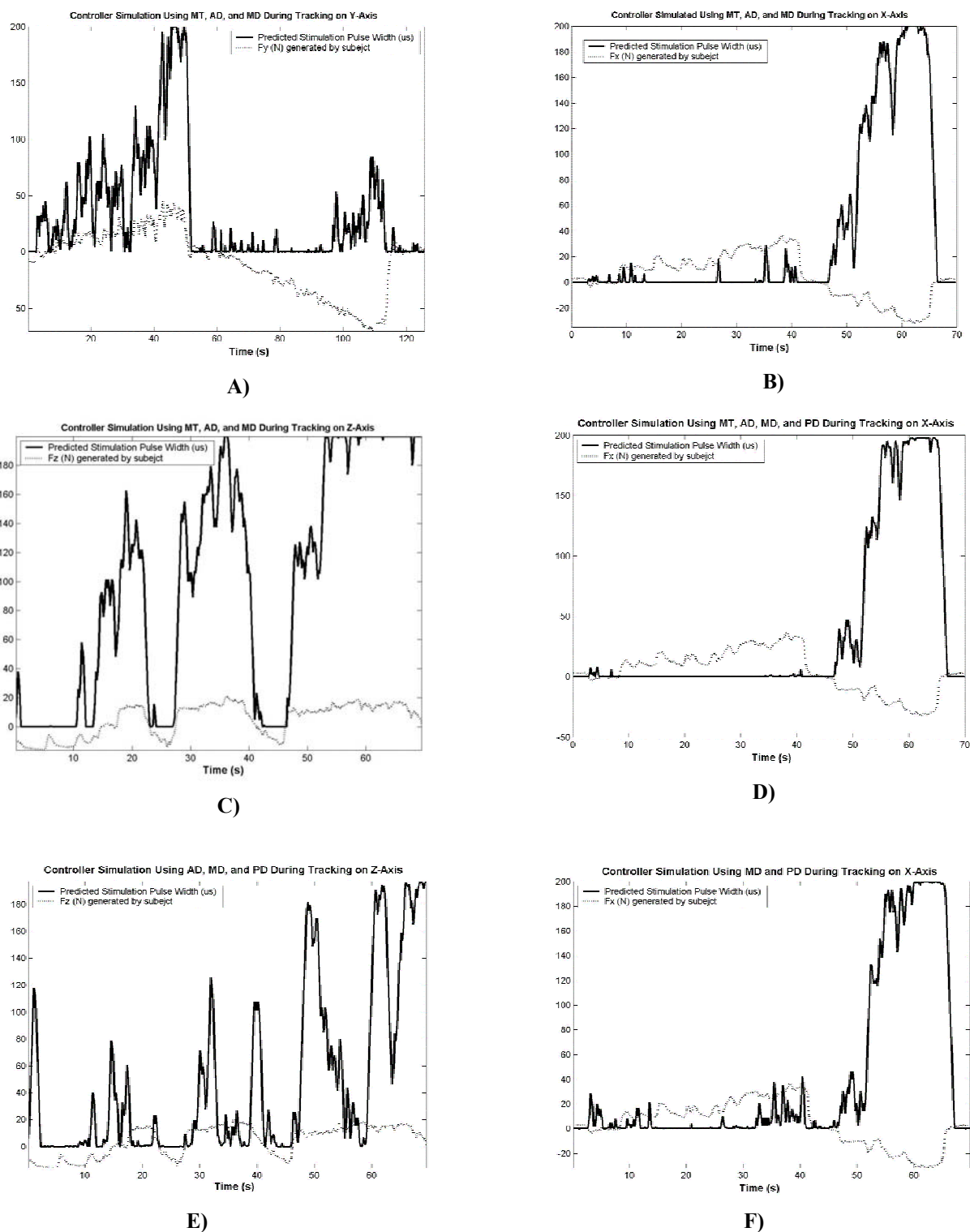
Neural Network Controller Simulations

Figure 17. Trained neural network controllers for subject 1were simulated with the data collected as subjects tracked goal endpoint force vectors along an axis during data collection.

25

Future Work

To this point, the controller has only been trained with data collected from one subject at one location in space. While the trained controller has been evaluated mathematically, it has yet to be tested for functional gains in a C5/C6 SCI subject. Therefore, data will be collected from four C5/C6 SCI subjects as described above. Data will be collected at three locations in space (Figure 12). Separate network controllers will be trained and evaluated as described above for each subject. After each subject has an ANN controller trained for them and the controller has been tested mathematically as described above, the controller will be implemented in the subject and tested functionally. We will test the subject for their range of isometric endpoint force vectors, stability of tracking discrete isometric endpoint force vectors, dynamic point-to-point endpoint tracking, and a few functional tasks such as overhead reach and eating. These functional tests will be evaluated using the synergistic controller and reciprocal control of triceps stimulation and the results will be compared.

References

Memberg, WD, Murray, WM, Ringleb, SI, Kilgore, KL and Snyder, SA,"A transducer to measure isometric elbow moments," Clin Biomech, 16: 918-920, 2001.